Absorption equilibrium and permselectivity of cation exchange membranes in sulfuric acid, sodium chloride and nickel sulfate media

ARTICLE *in* JOURNAL OF MEMBRANE SCIENCE · OCTOBER 2008

Impact Factor: 5.06 · DOI: 10.1016/j.memsci.2008.06.035

3 AUTHORS:

Xuan Tuan Le
MiQro Innovation Collaborative Centre
29 PUBLICATIONS **312** CITATIONS
SEE PROFILE

Claudine Buess-Herman
Université Libre de Bruxelles
86 PUBLICATIONS **1,353** CITATIONS
SEE PROFILE

Heinz Hurwitz
Université Libre de Bruxelles
65 PUBLICATIONS **752** CITATIONS
SEE PROFILE

Journal of Membrane Science 323 (2008) 288–298

Contents lists available at ScienceDirect

Journal of Membrane Science

journal homepage: www.elsevier.com/locate/memsci

Absorption equilibrium and permselectivity of cation exchange membranes in sulfuric acid, sodium chloride and nickel sulfate media

Le Xuan Tuan[a,b], C. Buess-Herman[a,*], H.D. Hurwitz[a]

[a] *Service de Chimie Analytique et Chimie des Interfaces (CHANI) – CP 255, Université Libre de Bruxelles, Campus de la Plaine, Bd. du Triomphe, 1050 Bruxelles, Belgium*
[b] *Service de Traitement des Eaux et Pollution – CP 208, Université Libre de Bruxelles, Campus de la Plaine, Bd. du Triomphe, 1050 Bruxelles, Belgium*

ARTICLE INFO

Article history:
Received 12 February 2008
Received in revised form 4 June 2008
Accepted 5 June 2008
Available online 21 June 2008

Keywords:
Ion-exchange membranes
Absorption equilibrium
Donnan equilibrium
Micro-heterogeneity
Selectivity
Ion mobility

ABSTRACT

Properties of the homogeneous cation exchange membranes CMS and CMV were investigated in order to assess the applicability of the model of micro-heterogeneous structure in the case of these membranes. Electrical conductivity measurements provide the volume fractions of the two distinct internal phases that are supposed to compose the entire membrane volume. These partial volumes as well as the membrane overall swelling depend on the nature of the external solutions. In order to extend our knowledge concerning the role of each of these phases, the absorption isotherms of H_2SO_4 and NaCl have been measured in relation to the membrane water content. We have determined experimentally a partition coefficient at absorption equilibrium between the external solution and the so-called interstitial phase. With the aim of clarifying the condition of validity of the Donnan theory in terms of the micro-heterogeneous model, we have developed a treatment involving a more detailed description of the water and salt distribution at equilibrium between the interstitial phase and the gel phase. This study accounts for the influence of different possible structural configurations of the poly-electrolyte macro-ions which are confined to the gel phase. The absorption properties of both membranes were also studied at equilibrium with a mixed $H_2SO_4 + NiSO_4$ solution. Application of conductivity measurements to these systems has led to determine the H^+ ion and Ni^{2+} ion mobility in both membranes and to bring out the comparison of these values in terms of the membrane internal structure.

1. Introduction

Rinse streams of metal finishing processes are usually concentrated in bivalent metal ions and frequently in strong acids. Disposals of these streams pose therefore important pollution problems. Some specific metal recovery methods are thus required to process these metal-laden rinse solutions and the use of electrodialysis is often considered as an appropriate technique. The application of electrodialysis may also enable to control and improve the quality of electroplating baths. The benefit of this methodology, with respect to the composition of these baths, is to reduce the need for their frequent replenishment. The recovery of acid from spent pickling baths by electrodialysis constitutes another procedure of considerable interest for the treatment of waste effluents. All these different industrial applications of electrodialys, in order to be feasible, require the use of some specific commercial cation exchanges membranes capable of removing efficiently either bivalent cations or acid or separating the acid from the salt. As reported in the literature, the Selemion CMV cation exchange membrane can be used to this end. The introduction of this membrane allows to remove and concentrate both sulfuric acid and nickel sulfate [1,2] but, because of its too low difference of permselectivity with regard to the hydrogen ion and the bivalent cations, this membrane does not produce a successful separation of these compounds. On the contrary, the Neosepta CMS cation exchange membrane displays a large permselectivity towards the hydrogen ion compared to the bivalent cations. It is thus successful in removing Ni^{2+} ions in presence of acid from metal-laden electroplating baths or washing acid solutions.

Some physical-chemical properties of both CMV and CMS membranes were investigated in two previous papers [3,4]. We characterized these membranes by determining their ion-exchange capacity, water content and conductivities at equilibrium with sulfuric acid solutions of various concentrations up to 3.00 M. As a whole, both membranes appear as homogeneous. They are ideally permselective with respect to the transport of hydrogen ions in

* Corresponding author. Tel.: +32 2 6502939; fax: +32 2 6502934.
E-mail address: cbuess@ulb.ac.be (C. Buess-Herman).

0376-7388/$ – see front matter © 2008 Elsevier B.V. All rights reserved.
doi:10.1016/j.memsci.2008.06.035

sulfuric acid media. On account of our experimental results we proceeded to define a model describing the internal structure of both membranes. We found that their behaviour is remarkable in two aspects. First, in presence of acids, in the case as well of H_2SO_4 as HCl, the membrane swelling is very large and passes trough a maximum at a given acid concentration of the equilibrating solution. Such maximum is absent in the case of a NaCl equilibrating solution. Second, measurements of the membrane conductivities have confirmed the validity of the model of micro-heterogeneous structure as proposed by Gnusin et al. [5] and later developed by Zabolotsky and Nikonenko [6,7]. Application of this theory brings about a two-phase representation of the electro-membrane microstructure. One phase, the so-called joined-gel phase, combines a poly-electrolyte gel and the stable inert polymer matrix. The other phase represents the aqueous interstitial solution that fills the inner parts of meso- and macro-pores, fissures and cavities of the membrane. By using this model in presence of acid solutions we succeeded to determine the volume fractions of these internal phases. The calculated interstitial phase volume fractions are however noticeably larger (20% and 29% in the case of respectively CMV and CMS) than accepted in the literature for the characterization of homogeneous ion-exchange membranes [8,9]. In our previous paper, such divergences in the case of homogeneous membranes were explained in terms of models relying on the formation inside the gel phase of specific poly-electrolyte macro-ion domains. We considered the fact that the partial volumes and conformations, from stretched state to denser coiled configuration, of these poly-electrolytes are determined by the nature of the counter-ions and the amount of electrolyte absorbed in the interstitial phase and therefore depend sharply on the presence of H^+.

In their treatment, Zabolotsky and Nikonenko supposed similar compositions of the external equilibrating solution and internal interstitial solution. In our previous study, with respect to this point, we assumed a concentration difference at partition equilibrium of the electrolyte between the external equilibrating solution and interstitial solution. We established experimentally such partition in the case of the CMV membrane at equilibrium with H_2SO_4 and NaCl. As a consequence of this partition, the Donnan exclusion of co-ions in the membrane is not any more applicable to the overall membrane system. Actually, this Donnan exclusion still exists but is relegated to the absorption equilibrium existing across the micro-interfaces distributed inside the membrane between the interstitial and joined-gel phases.

With the aim of clarifying the application of the Donnan theory to the membrane system under the conditions of validity of the micro-heterogeneous model, we endeavour, in the present work, to determine the equilibrium compositions of the interstitial phase and joined-gel phase in the case of the CMS ion-exchange membrane in presence of acid and salt solutions. Considering the difference of selectivity of the CMV and CMS membranes towards the hydrogen ion and a bivalent metallic cation [2,10], we wish also to devote our study to the equilibrium properties of these two membranes in contact with a mixed $H_2SO_4 + NiSO_4$ solution. The application of conductivity measurements to these systems will lead to derive the values of the hydrogen ion and the cation mobility in these membranes and brings out the comparison of these values in terms of the membrane fabrication characteristics.

2. Experimental methods

2.1. The characteristics of ion-exchange membranes

Some main characteristics of CMV and CMS membrane samples used in our present study are given in Table 1. The measurements were performed as indicated in previous articles [3,4] where all methods of determination were thoroughly described. The exchange capacity C_{ex} is given in mequiv./g of dry membrane and the densities ρ_d and ρ_m of respectively the dry and wet membranes are expressed in g/cm^3.

Table 1
Type of ion-exchange membrane and their characteristics

Name	Selemion CMV	Neosepta CMS
Type	Cation	Cation
Thickness (mm)	0.140–0.145	0.145–0.150
Exchange capacity C_{ex} (mequiv./g)	1.95 ± 0.05	2.20 ± 0.05
Water content (%)	18–28	22-30
Structure property	PS/DVB	PS/DVB
Transport number of H^+	1.00	1.00
Transport number of Na^+	0.98	0.97
Charged group	Sulfonate	Sulfonate
Backing	PVC	PVC
Density of dry membrane ρ_d (g/cm^3)	1.15 ± 0.10	1.16 ± 0.10
Density of wet membrane ρ_m(g/cm^3)	1.20 ± 0.10	1.20 ± 0.10

2.2. The membrane conductivity

The electric resistances at 25 °C of membrane samples, previously equilibrated in sulfuric acid solutions of given concentrations, were obtained from the membrane impedance diagrams plotted in a range of frequencies extending from 1 Hz to 100 kHz. The alternating current was supplied to a two-compartment mercury electrode cell [3]. Measurements were performed with a SOLATRON 1250 frequency analyzer equipped with an electrochemical interface. Details concerning this technique are given in Refs. [11–13]. The specific conductivity κ^m of the membrane is calculated by using the relation:

$$\kappa^m = \frac{d}{RA} \quad (1)$$

where R is the membrane resistance and d and A are respectively the thickness and the exposed membrane area ($A = 0.866\ cm^2$) in the two-compartment mercury electrode cell. The determination of R is straightforward from the membranes Argand plots that present a typical shape as shown in Fig. 1.

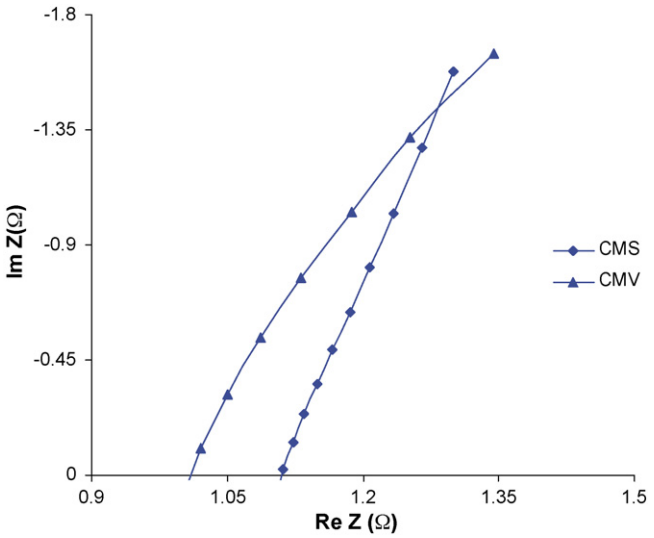

Fig. 1. Impedance diagrams of the CMV and CMS membranes soaked in a 0.25 M sulfuric acid solution.

2.3. Determination of the absorbed amount of electrolyte

Three membrane samples were left to soak each during 24 h at 25 °C in solutions at different acid or salt concentrations. Dry weight W_b of these samples was known. After wiping up the solution deposited on the membrane surface, the membranes were immersed into sufficiently large amounts of distilled water at 25 °C during 24 h for complete desorption of the H_2SO_4 or salt. A HP-1050 ion chromatography (column AG 144-mm) and AAS were used to determine respectively the quantity of H_2SO_4 and NaCl released by the membrane. Tests were performed after this immersion to control the presence of remaining acid or salt in the membrane. A second immersion of the membrane did not allow detecting in the case of 2.00 and 3.00 M acid or electrolyte solutions more than faint amounts of residual absorbed acid or salt at concentrations below the limit of error of the analytical technique.

2.4. Ion-exchange equilibrium

Previous experimental studies in the laboratory have proved that the time necessary to reach the stable state of absorption of acid could be more than 16 h, depending on the history of the CMV and CMS membrane samples. On account of these results, the membranes were first immersed in 0.5 N H_2SO_4 solutions for 24 h. After wiping up the sulfuric acid settled on the membrane surface, the membranes were equilibrated in H_2SO_4/$NiSO_4$ solution for 24 h under stirring condition. The membranes were removed from the solution and their surface was wiped up again before immersion in 50 ml NaCl 1 M solution for 24 h in order to disgorge all the hydrogen and nickel ions. Acid–base titration and atomic absorption spectroscopy were used for determination of respectively the amounts of acid and nickel ions released in this solution.

3. Results and discussion

3.1. Membrane swelling in relation to membrane micro-heterogeneity

The membrane water content is defined as follows:

$$W = \frac{W_a - W_b}{W_b} \quad (\text{g H}_2\text{O/g dry membrane}) \qquad (2)$$

where W_a and W_b denote respectively the weight of the wet and dry membranes.

We found in our previous investigation [3,4] that the water content of CMV and CMS membranes passes through a maximum at a concentration of sulfuric acid of about 0.5 M (Fig. 2). The degree of swelling changes from 0.19 ± 0.02 and 0.25 ± 0.02 in pure water for the CMV and CMS membranes up to 0.23 ± 0.02 and 0.29 ± 0.02 at the maximum. We have plotted in the same Fig. 2 the values of membrane swelling obtained at equilibrium with HCl and NaCl solutions. We obtained, in the case of HCl, behaviour similar to that observed with H_2SO_4. However, the water content is larger than in the case of H_2SO_4. Such difference between these two systems remains after the maximum. In the case of membranes treated with NaCl, after an initial decrease as a function of the equilibrating solution concentration, the membrane swelling reaches a plateau extending up to about 1 M. This is followed in the range of higher concentrations by a monotonous decrease of water content.

In order to explain these results, a model was devised in connection with the chemical-physical properties of poly-electrolytes [3]. Polystyrene sulfonate domains were described with regard to their conformation as a function of Coulombic interaction and osmotic effects. In presence of acid, it was suggested that a network of hydrated counter-ionic groups of structures of the type

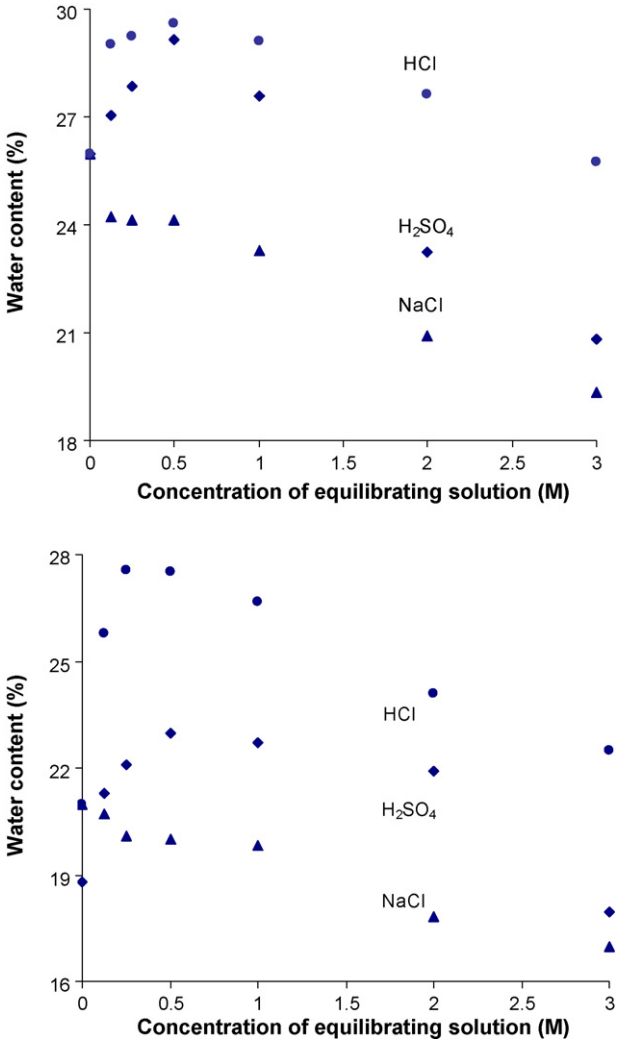

Fig. 2. Water content of the membrane as a function of the equilibrium solution concentration (at 25 °C) for HCl, H_2SO_4 and NaCl solutions: (a) CMS; (b) CMV.

$H_5O_2^+$ or $H_9O_4^+$ can be formed inside the poly-ions [3]. These are tightly bound to individual sulfonate sites fixed on the polystyrene sulfonate chains. By this way they are screening the negative charges distributed along the polymer chain and thus decreasing the Coulombic repulsion. This leads to a dense coiled configuration of the macro-ions. As a further consequence of the high degree of the poly-electrolyte electric neutralization one may expect a decrease of the osmotic pressure exerted in the macro-ion and thus some further shrinking of the poly-electrolyte domains. On the contrary, in presence of NaCl, hydrated Na^+ counter-ions are in average weakly bound to the individual charged sulfonate groups and are freer to move inside the macro-ions. As a consequence, the Coulombic repulsion along the polymer chains is enhanced and the macro-ions keep therefore a relative open structure, more similar to a rod-like polymer configuration.

In the model of internal micro heterogeneity, the membrane is described as composed of a joined-gel phase and an interstitial phase (Fig. 3). The joined-gel phase combines the membrane inert polymer matrix and a poly-electrolyte pure gel phase. The latter consists of a relatively uniform distribution of hydrated ionogenic groups corresponding to the hydrophilic parts of the polymer impregnated with water and surrounded by hydrated counter-ions. The interstitial phase on the other hand is made out of an electro-

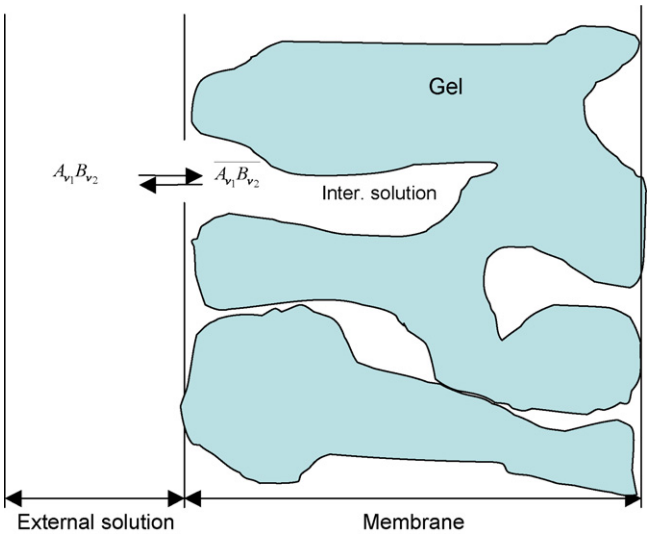

Fig. 3. Model of internal micro-heterogeneity.

neutral solution filling the interstices between the elements of the gel phase [6,7].

Since the joined-gel phase contains, by definition, the macro-ionic domains, it becomes clear that the presence of hydrated H^+ counter-ions has the effect of shrinking the gel phase and thus enhancing the partial volume of the interstitial phase. As a result, the membrane water content will be increased at membrane equilibrium with acid as compared to the situation obtained in the case of equilibrium with NaCl. As suggested in Ref. [3], the appearance of a swelling maximum as a function of the acid concentration can be related to the opposed influences, on the one hand, of the poly-ion coiled structure shifting to dense configurations that prevents any further introduction of acid and water in the macro-ion domains and, on the other hand, of the diminishing osmotic drive of water from the external solution into the interstitial phase. The increase of swelling is larger at equilibrium with HCl than with H_2SO_4. Actually, in acid media the presence of Cl^- entails a denser macro-ion configuration of the poly-electrolyte domains than the presence of SO_4^{2-}. Such result was discussed [3] in terms of the property of Cl^- to be repelled from the inside of the macro-ion space because its peripheral hydration is less compatible than that of the sulfate ion with the organisation of water structure induced by the H^+ counter-ion hydration.

In the theory of Zabolotsky and Nikonenko [6,7], the two phases of the micro-heterogeneous model are characterized by volume fractions defined as follows:

$$f_1 = f_1' + f_{in} \tag{3}$$

$$f_1 + f_2 = 1 \tag{4}$$

where f_1 is the volume fraction of the joined-gel phase; f_1' is the volume fraction of the pure gel phase; f_{in} is the volume fraction of the inert phase; f_2 is the volume fraction of the interstitial phase.

It is worth noting that the values of f_2 and W given in Table 2 and the swelling depicted in Fig. 2 are much larger for CMS than for CMV membranes. These results may rely on the fact that the cross-linking of polystyrene is more important in CMS than in CMV membranes. Such fabrication characteristic entails a larger rigidity of the poly-electrolyte domains. It may thus be expected, according to the foregoing consideration about the micro-heterogeneity, that this cross-linking reduces the gel phase partial volume and as a consequence, enhances the interstitial phase partial volume and the membrane overall water content.

Table 2
Water absorption in the membrane as estimated in Ref. [3,4]

		CMV membrane	CMS membrane
In contact with H_2SO_4 solution (0–0.05 M)	W (%)	20	26
	f_2 (%)	20	29
In contact with NaCl solution (0–1 M)	W (%)	≈20	≈26
	f_2 (%)	10	13

3.2. The absorption of acid and salt

Many determinations of co-ion absorption in ion-exchange membranes can be found in the literature (see, e.g. [12,14,15]). Such evaluation is of particular importance for the understanding of both the mechanism of Donnan exclusion and the ion transport process across the membrane. It has been recognized that the amount of co-ions co-absorbed is a reflection of the particular type of interactions between co-ions and counter-ions induced by the hydrophobic or hydrophilic membrane properties, for example of ion pairing or complex formation, and that at the end such interactions influence drastically the membrane permselectivity. The number of absorbed acid molecules per site as a function of the concentration of the external acid solution is shown in Fig. 4. The experimental value of the absorbed acid molality $\bar{m}_{exp}$ is given by:

$$\bar{m}_{exp} = \frac{1000}{18} \times \frac{\bar{N}_{H_2SO_4}}{\bar{N}_{H_2O}} \tag{5}$$

where $\bar{N}_{H_2SO_4}$ is the number of absorbed acid molecules per site and $\bar{N}_{H_2O}$ is the number of water molecules per site. The values $\bar{m}_{exp}$ are displayed in Fig. 5 as a function of the acid molality m_S of the external solution. In Figs. 4 and 5, we have also recorded the values of $\bar{N}_{NaCl}$ and $\bar{m}_{exp}$ obtained at equilibrium with an external NaCl solution. For comparison, we have included in these figures the plots for CMV measured in our previous work [3,4].

The values of $\bar{m}_{exp}$ shown in Fig. 5 vary linearly with m_S. Thus, the equilibrium between the membrane and the external solution can be expressed by a partition equilibrium coefficient $\tilde{K}$ defined such as

$$\frac{\bar{m}_{exp}}{m_s} = \tilde{K} \tag{6}$$

We get from Fig. 5, the values $\tilde{K} = 0.045$ for H_2SO_4 and 0.70 for NaCl in the CMV membrane and $\tilde{K} = 0.11$ for H_2SO_4 and 0.47 for NaCl in the case of the CMS membrane.

In Figs. 4 and 5 we observe that, in the case of both membranes, the absorbed amount of acid is smaller than the absorbed amount of salt. Our discussion with regard to the results shown in Fig. 2 leads to suggest that the differences of electrolyte absorption, just like the case of water content, could be caused by the counter-ions H^+ and Na^+. In fact, in presence of Na^+, the poly-ion chains in the joint gel phase are extended in length. Consequently the polystyrene domains are more open and less dense. They might thus accommodate a larger amount of co-ions and counter-ions partially distributed inside ionic clouds that neutralize the fixed charged groups. As shown below in this paper, the number of co-ions absorbed in the gel joined-gel phase remains however too small as to explain the large difference between $\bar{N}_{H_2SO_4}$ and $\bar{N}_{NaCl}$ only on the basis of such ionic process. The effects of the Cl^- anion mono- and SO_4^{2-} double charge on the absorption were considered in Ref. [3]. There we calculated the heterovalent ion Donnan inclusion whereby the amount of sorbed solute in the

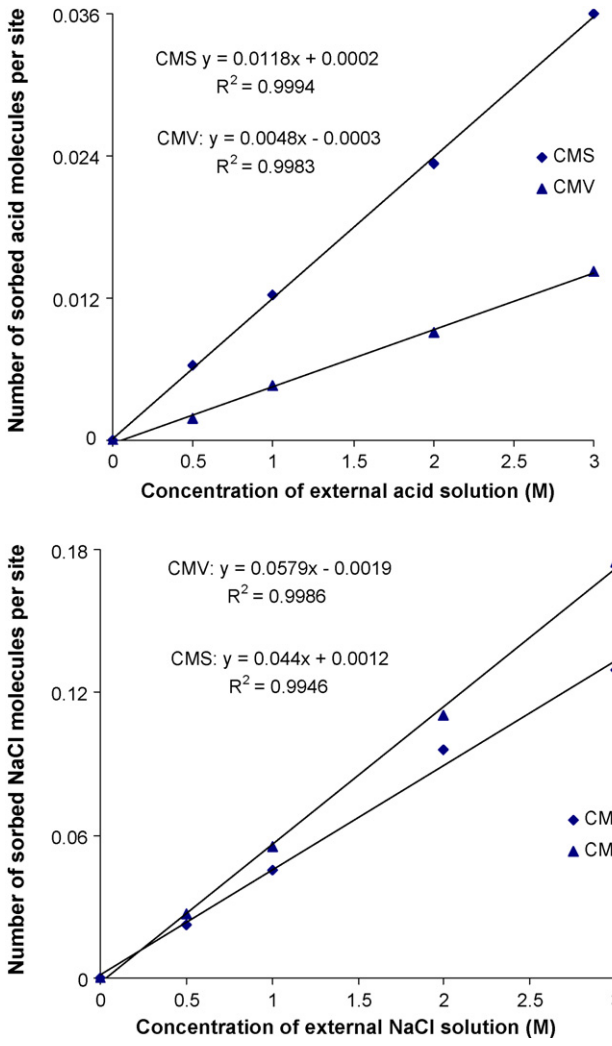

Fig. 4. Number of absorbed electrolyte molecules per sites, N_s, as a function of external electrolyte concentration in the case of H_2SO_4 (a) and NaCl (b).

membrane decreases with the increase of the co-ion valence even though the electrolyte molality in the exchange solution remains constant. It was shown that such valence effect between Cl^- and SO_4^{2-} is unable to explain the large difference of m_{exp} depicted in Fig. 4 for both ions. We have further insisted on the total discrepancy between the experimental data for $\bar{m}_{exp}$ and those calculated with the Donnan theory. The absorption differences illustrated in Figs. 4 and 5 for the acid and salt will have to be treated, as indicated next, in the case of NaCl, by taking into consideration some specific partition of the electrolyte at equilibrium between the external solution and interstitial phase.

3.3. Distribution of absorbed electrolyte in the membranes

In terms of the model proposed by Zabolosky and Nikonenko [6], the Donnan equilibrium should be relegated to the interface region between interstitial and gel phases. In view of such application of the Donnan theory, we consider the case of a 1–1 electrolyte: $AB \rightarrow A^+ + B^-$.

We may thus suppose that:

$$\frac{\bar{m}'_{1+} * \bar{m}'_{1-}}{\bar{m}_{2+} * \bar{m}_{2-}} = \bar{K}_{gel} \quad (7)$$

where $\bar{m}_{2i}$ and $\bar{m}'_{1i}$ stand for the i ion molality respectively in the interstitial phase and in the pure gel phase.We may further express the equilibrium between the interstitial phase and the joint-gel phase as follows:

$$\frac{\bar{c}_{1+} * \bar{c}_{1-}}{\bar{c}_{2+} * \bar{c}_{2-}} = \bar{k}_{gel} \quad (8)$$

where $\bar{c}_{2i}$ and $\bar{c}_{1i}$ designate respectively the i ion concentration in the interstitial phase and in the joined-gel phase.

To resolve the problem, we follow the usual procedure which consists in setting the conditions of electroneutrality in both phases. Thus, we get in the joined-gel phase

$$\bar{c}_{1-} = \bar{c}_{1+} - \bar{c}_{1ex} \quad (9)$$

where $\bar{c}_{1ex}$ represents the equivalent of fixed charges per cm^3 in this phase at absorption equilibrium:

$$\bar{c}_{1ex} = \frac{\rho_m C_{ex}}{f_1(1+W)} \quad (10)$$

By definition, in the interstitial phase one gets

$$\bar{c}_{2+} = \bar{c}_{2-} \quad (11)$$

The solution of Eq. (8) with conditions (9) and (11) yields the values of local concentration at Donnan equilibrium between the

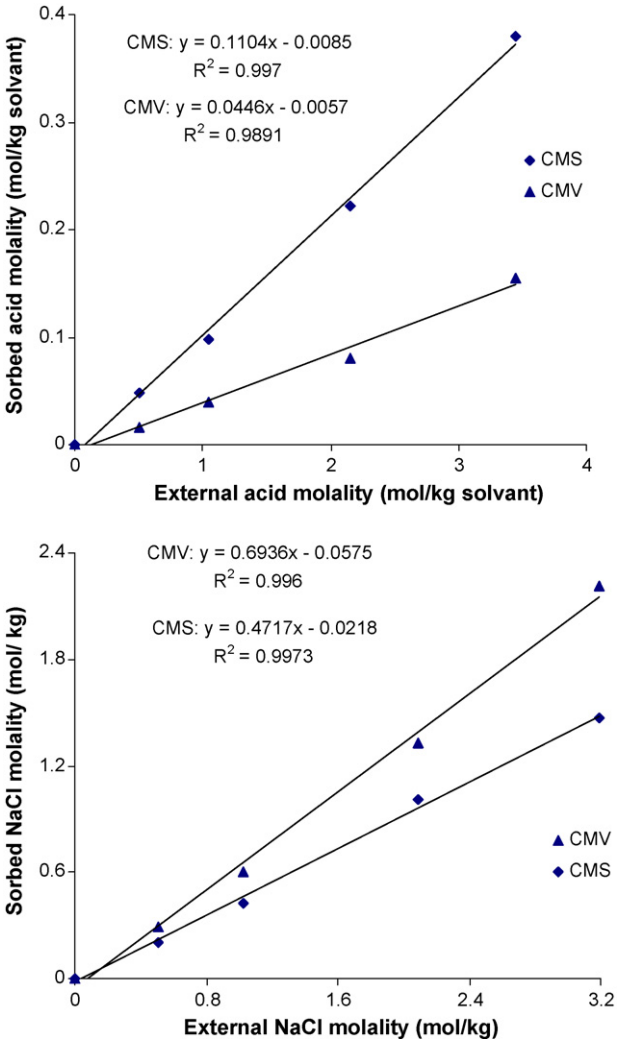

Fig. 5. Molality of the absorbed electrolyte, $\bar{m}_{exp}$, as a function of the external electrolyte molality: (a) H_2SO_4; (b) NaCl.

interstitial phase and the joined-gel phase. One finds the classical expression:

$$\frac{\bar{c}_{1-}}{\bar{c}_{2-}} = -\frac{\bar{c}_{1ex}}{2\bar{c}_{2-}} + \sqrt{\left(\frac{\bar{c}_{1ex}}{2\bar{c}_{2-}}\right)^2 + \bar{k}_{gel}} \tag{12}$$

Let us next introduce the condition of mass balance in the membrane:

$$\frac{\bar{N}_s C_{ex}\rho_m}{(1+W)} = \bar{c}_{1-}\left(\frac{W\rho_m}{(1+W)\rho_w} - f_2\right) + \bar{c}_{2-}f_2 \tag{13}$$

where, $\bar{N}_s$ denotes the total number of moles of electrolyte absorbed in the membrane per equivalent of fixed charges and ρ_w is the density of water supposed to be equal to $\rho_w = 1$. In this expression, the first term of the right-hand side gives the number of moles of absorbed electrolyte in the joined-gel phase per cm^3 of the wet membrane and the second term is the number of absorbed electrolyte in the interstitial phase per cm^3 of the wet membrane.

We intend to determine next the number of moles of electrolyte absorbed in the interstitial phase per equivalent of fixed charge $\bar{N}_{2S}$:

$$\bar{N}_{2s} = \frac{\bar{c}_{2-}f_2(1+W)}{\rho_m C_{ex}} \tag{14}$$

Upon introduction of Eq. (12) into Eq. (13) and taking into account the definition of $\bar{N}_{2S}$, one obtains:

$$\bar{N}_s = \left(-\frac{1}{2f_1} + \sqrt{\left(\frac{1}{2f_1}\right)^2 + \left(\frac{\bar{k}_{gel}}{f_2}\right)^2 \bar{N}_{2s}^2}\right)\left(\frac{W\rho_m}{(1+W)\rho_w} - f_2\right) + \bar{N}_{2s} \tag{15}$$

The following inequality is usually satisfied in the systems under investigation,

$$\left(\frac{\bar{k}_{gel}}{f_2}\right)^2 \bar{N}_{2s}^2 << \left(\frac{1}{2f_1}\right)^2 \tag{16}$$

With respect to this inequality, we expand in series the square root in Eq. (15), keeping the term of first order. One gets

$$\bar{N}_s = \left(\frac{\bar{k}_{gel}}{f_2}\right)^2 f_1\left(\frac{W\rho_m}{(1+W)\rho_w} - f_2\right)\bar{N}_{2s}^2 + \bar{N}_{2s} \tag{17}$$

This quadratic equation is solved in order to obtain an expression of $\bar{N}_{2S}$

$$\frac{\bar{N}_{2s}}{\bar{N}_s} = \frac{\sqrt{1 + 4\bar{N}_s(\bar{k}_{gel}/f_2)^2 f_1(W\rho_m/(1+W)\rho_w - f_2)} - 1}{2\bar{N}_s(\bar{k}_{gel}/f_2)^2 f_1(W\rho_m/(1+W)\rho_w - f_2)}$$

$$= 1 - \bar{N}_s\left(\frac{\bar{k}_{gel}}{f_2}\right)^2 f_1\left(\frac{W\rho_m}{(1+W)\rho_w} - f_2\right) + O(\bar{N}_s^2)\ldots \tag{18}$$

As noted before, W and $\bar{N}_s$ are known experimental values and f_2 is derived from electric conductivity measurements. It is thus possible to calculate by means of Eq. (18) the fraction of absorbed molecules in the joined-gel phase $(\bar{N}_s - \bar{N}_{2s})/\bar{N}_s$.

Because of both the inaccuracy in the determination of ρ_m and the very small absorption of acid in the joint-gel phase, the application of Eq. (18) to the case of acid absorption does not allow a valid estimate of $\bar{N}_{2S}$. For H_2SO_4 the problem becomes even more complex because of the difficulty to decide about the role played by the second acid dissociation step in the membrane. Such difficulties of calculating $\bar{N}_{2S}$ are not encountered in the case of NaCl absorption.

The determination of the coefficient $\bar{k}_{gel}$ poses also some problem. In Ref. [3] a relation was established between the Donnan constant $\bar{K}_{gel}$ and $\bar{k}_{gel}$. By adopting the same arguments as in Ref. [16] and taking into account the definition of parameters used in the foregoing demonstration, the following expression was derived [3,16]

$$\bar{k}_{gel} = \bar{K}_{gel}\left(\frac{\rho_m(W/(1+W)) - \rho_w f_2)}{1 - f_2}\right) \tag{19}$$

In the classical Donnan model $\bar{K}_{gel}$ is usually set equal to unity. Notwithstanding the doubts we have raised in Ref. [3] about the validity of this assumption in our system, we have kept, like in Ref. [6], the value $\bar{K}_{gel} = 1$.

In the Table 3, we have recorded a rough estimate (±10%) of the values of $\bar{N}_s - \bar{N}_{2s}/\bar{N}_s$ at the equilibrium state between the membrane and a NaCl 1.0 M solution. We calculated also the fraction of water absorbed in the joined-gel phase. This has been written as W_1/W and by definition is given by

$$\frac{W_1}{W} = 1 - \frac{\rho_w f_2(1+W)}{\rho_m W} \tag{20}$$

The fraction of absorbed NaCl in the joined-gel phase, which is, according to the model equivalent to the fraction present in the pure gel phase, is about 0.5% in the CMV membrane and 0.2% in the CMS membrane. As for the fraction of water absorbed under the same conditions in the gel phase, it amounts approximately to 50% in the CMV membrane and is somewhat less, thus about 40% in the CMS membrane. Again, it may be noted that the increased cross-linking in CMS determines a lower relative salt content in the macro-ion domains compared to the case of CMV. The results derived in Table 3 involve the existence of a rather equal distribution of water in the membrane at equilibrium amongst the interstitial and gel phases. This property is understandable in relation to the open structure taken by the poly-ion chains under the condition that the macro-domains in the gel are electrically neutralized by Na^+ counter-ions.

With respect to the content of electrolyte and water in the interstitial phase, we are now in position to evaluate the partition coefficient $\tilde{K}_{int.}$ corresponding to the distribution equilibrium between the external solution and the interstitial phase

$$\frac{\bar{m}_{2s}}{m_s} = \tilde{K}_{int} \tag{21}$$

where $\bar{m}_{2s}$ is the molality of the absorbed electrolyte in the interstitial phase.

By application of definitions given in Eq. (6), (14) and (20) one finds

$$\tilde{K}_{int} = \left(\frac{\bar{N}_{2s}}{N_s}\right)\left(\frac{\tilde{K}}{1 - (W_1/W)}\right) \tag{22}$$

Since the ratio $\bar{N}_{2s}/N_s$ is nearly equal to one, we obtain for NaCl, with the values recorded in Table 3 and those plotted in Fig. 5, that $\tilde{K}_{int}$ becomes equal to 1.4 ± 0.2 and 0.8 ± 0.1, respectively for CMV and CMS. The study of equilibrium condition of solute distributed between bulk and interfacial water or water sorbed in porous media (without fixed ion sites) has led, as in the case of chromatographic application or reverse osmosis, to relate such partition coefficients to effects associated with the hydrophobicity of the polymer material and the accessibility of narrow pores to the solute particles. We cannot exclude some important imprecision in the determination of $\tilde{K}_{int}$, due as well to the choice of $\tilde{K}_{gel} = 1$ as to experimental errors and model deficiencies; nor is there, however, any theoretical reason to expect $\tilde{K}_{int}$ to be exactly equal to unity. Due to the influence of the pore walls and the matrix network inside the membrane interstitial phase, water may have a less cooperative structure, i.e., may be, on the average, hydrogen

Table 3
Determination of the fraction of absorbed electrolyte molecules in the gel phase

		Molality of sorbed electrolyte (mol/kg solvant)	$\bar{N}_s$	W	f_2	$(\bar{N}_s - \bar{N}_{2s})/\bar{N}_s$	W_1/W
In NaCl 1 M	CMV	0.69	0.058	0.20	0.10	0.5×10^{-2}	0.5
	CMS	0.47	0.044	0.23	0.13	0.2×10^{-2}	0.4

bonded to fewer other water molecules than in the dilute aqueous solution. Since the Cl^- ion is known to act as a disturbing centre for the bulk water structure, thus producing a net structure disordering effect, it is susceptible to get involved in a more stable interaction with water and a state of ion pairing with Na^+ in this phase. Such type of distribution effects, linked to so-called water structure induced ion interactions, are well known in aqueous solution electrochemistry. The higher cross-linking, producing rigidity and steric hindrance in the CMS membrane, could be the cause of a smaller partition coefficient in CMS membranes than in CMV membranes. In CMS membranes more water may be trapped in meso-, micro- and nano-pores where the accessibility of large Cl^- ions and hydrated Na^+ ions is reduced or where there is no room available for a complete ion hydration shell. By similar reasons of water structure induced interaction, the strongly hydrated and water-structuring SO_4^{2-} and H^+ ions will be hindered to absorb in the interstitial phase.

3.4. Exchange equilibrium of hydrogen and nickel ions in the membranes

Our investigation of membrane absorption properties in presence of sulfuric acid has been extended to the case of H_2SO_4 0.5 N solutions in presence of different concentrations of nickel sulfate. The C_{ex} values determined by means of separate experiments [1,16] for the two types of membranes selected for this study are quite similar. We obtained for the CMV membrane 2.15 mmol per g of dry membrane and for the CMS membrane 2.20 mmol per g of dry membrane with an estimated error of 5%. The quantity of H^+ and Ni^{2+} equivalents inside the membranes at absorption equilibrium are shown in Fig. 6 as a function of the $NiSO_4$ normality in H_2SO_4 0.5 N solution. Within the error margin of 5%, the measurements yield a sum of H^+ and Ni^{2+} equivalents per g. of dry membrane equal to the value of the ion-exchange capacity C_{ex}.[1] In the concentration range used in this study, Donnan co-ion inclusion can thus be considered as negligible.

In order to express the ion-exchange isotherms between the external solution and the membrane we define the equivalent ratios $x_{M^{2+}}$ in the equilibrating solution and $\bar{x}_{M^{2+}}$ in the membrane for the H^+–Ni^{2+} system as follows:

$$x_{Ni^{2+}} = \frac{2c_{Ni^{2+}}}{2c_{Ni^{2+}} + c_{H^+}} \quad \text{and} \quad \bar{x}_{M^{2+}} = \frac{2\bar{c}_{Ni^{2+}}}{2\bar{c}_{Ni^{2+}} + 2\bar{c}_{H^+}} \tag{23}$$

where $c_{m^{2+}}$ and $\bar{c}_{M^{2+}}$ are the ion concentrations (mol/cm^3) respectively in the solution and in the membrane. The recorded ion-exchange isotherms are depicted in Fig. 7. It is observed that the amount of absorbed nickel in the CMV membrane is slightly larger than in the CMS membrane.

Actually, with an external solution containing an equivalent ratio of nickel of 0.5 we get an equivalent ratio of absorbed Ni^{2+} of about 0.94 in the CMV and 0.89 in the CMS membrane.

3.5. Ionic mobility

The problem of competing transport between monovalent and bivalent ions across ion-exchange membranes was treated during the 10 last years by several authors [16–21]. The respective permselectivity towards H^+ and Ni^{2+} depends to a great extent on these ions relative amount inside the membrane and on these ions mobility during their transport inside the membrane. Different methods have been used to measure the ionic mobility in electro-membranes. In this work, we have studied the mobility of hydrogen ion and nickel ion in the CMV and CMS membranes

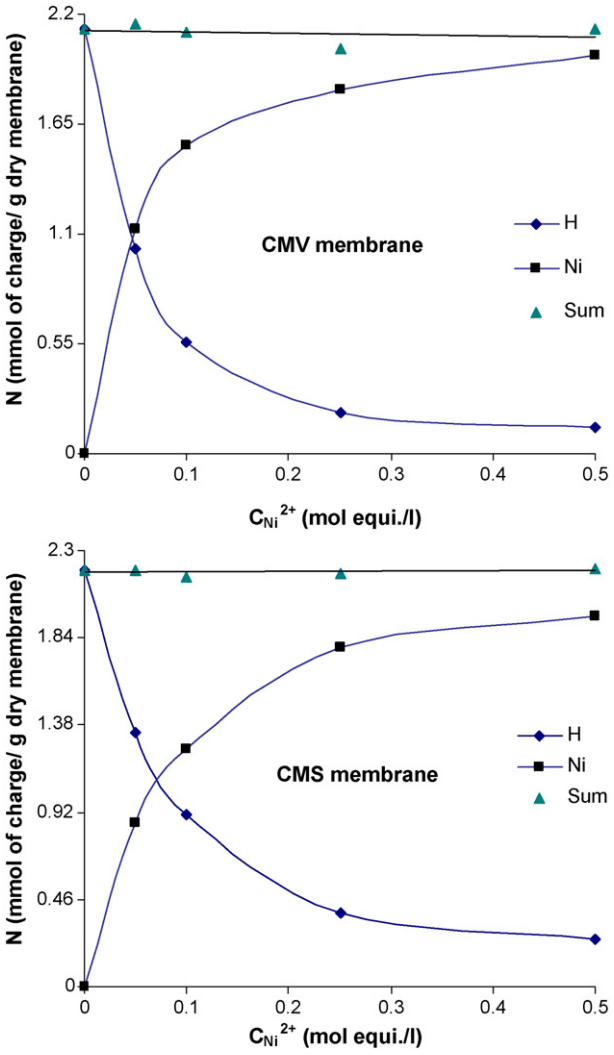

Fig. 6. Ion-exchange property and selectivity of the membranes:(a) CMV; (b) CMS.

[1] In the worst case for retention of electrolyte in the interstitial phase, it means at the maximum of water absorption in the CMS membrane, we get an amount of water of about 0.27 g per g of dry membrane for H_2SO_4 0.5 N (Fig. 2). For this concentration the normality of absorbed acid is about 0.0 5N as shown in Fig. 5. If we assume that all this water is in the interstitial phase and the density is equal to one, we find roughly $(0.27 \times 0.05) = 0.015$ mequivalent of cations in the interstitial phase per g of membrane as compared to 2.2 mequivalent/g for the exchange capacity. If we take the case of NaCl 0.5 M, assuming a partition constant equal to one, $f_2 = 0.10$, we get $0.10 \times 0.5 = 0.05$ mequiv./g which still remains below 5% of the exchange capacity. By using similar arguments, the values obtained with Ni^{2+} ions are probably between those of NaCl and H_2SO_4.

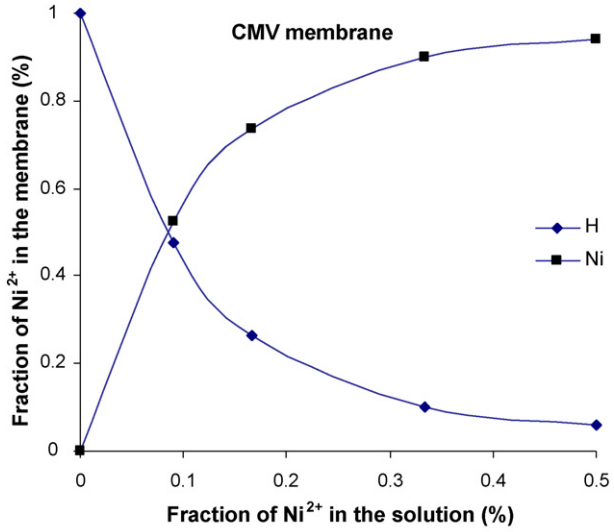

Fig. 7. Equivalent fraction of hydrogen and nickel ions in the membrane vs. the equivalent fraction of nickel ions in the equilibrating solution: (a) CMV; (b) CMS.

by means of membrane conductivity measurements. Considering the Hg cell experimental set-up for the impedance measurements, the admittance determined from Fig. 1 by extrapolation at high frequencies, accounts only for the ion conductivity inside the membrane without the influence of the membrane surface. This result can be rationalised with respect to the equivalent electrical circuit used to represent the electrochemical system. In this circuit the two working electrodes and the adjacent hydrated membrane surfaces operate all together as one component combining a capacitance and a resistance in parallel. This component is arranged in series with a resistance associated to the ionic conductivity displayed by the membrane. At high frequencies this resistance becomes the only measurable element.

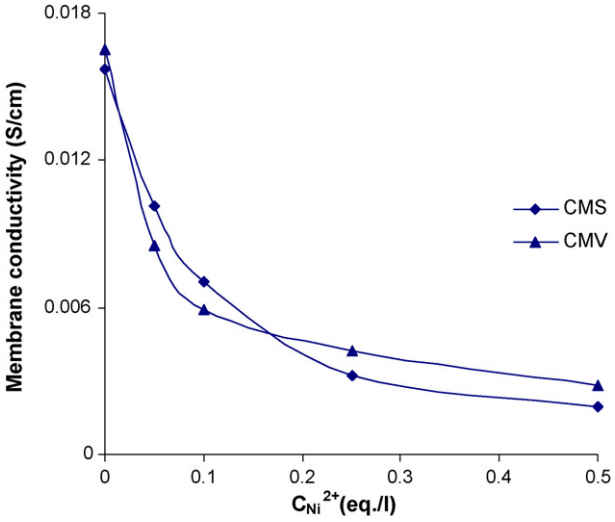

Fig. 8. Membrane conductivity vs. the equivalent concentration of Ni^{2+} in the equilibrating solution.

Fig. 8 displays the electrical conductivity of CMV and CMS membranes measured at equilibrium at 25 °C in a solution 0.5 N H_2SO_4 containing $NiSO_4$ at various concentrations. The membrane thickness under such conditions is respectively 0.0145 and 0.0150 cm for CMV and CMS. The apparent specific conductivity κ^m of the membrane can be expressed as follows:

$$\kappa^m = \sum_i z_i \bar{c}_i \bar{u}_i F \tag{24}$$

where $\bar{u}_i$ is the conventional mobility ($cm^2/s\,V$), $\bar{c}_i$ is the overall concentration of species i in the membrane phase (mol/cm^3).

In the case of the system under study, we may write that

$$\kappa^m = (\bar{c}_{H^+}\bar{u}_{H^+} + 2\bar{c}_{Ni^{2+}}\bar{u}_{Ni^{2+}} + 2\bar{c}_{SO_4^{2-}}\bar{u}_{SO_4^{2-}})F \tag{25}$$

With the condition of balance of charges, we get

$$\bar{c}_{H^+} + 2\bar{c}_{Ni^{2+}} = \bar{c}_{ex} + 2\bar{c}_{SO_4^{2-}} \tag{26}$$

with $\bar{c}_{ex}$ representing the number of equivalents of fixed charge per cm^3, thus given in mol equiv./cm^3.

From (24), (25) and (26), one readily obtains that:

$$\kappa^m = 2F(\bar{u}_{M^{2+}} - \bar{u}_{H^+})\bar{c}_{M^{2+}} + F\bar{c}_{ex}\bar{u}_{H^+} + 2F\bar{c}_{SO_4^{2-}}(\bar{u}_{SO_4^{2-}} + \bar{u}_{H^+}) \tag{27}$$

The last right-hand side term of Eq. (27) corresponds to the contribution of absorbed acid. Because the absorption isotherms have proved that the absorbed amount of acid is negligible (see also Table 4), we may just drop this term and write κ^m in the form

$$\kappa^m = F\bar{c}_{ex}(\bar{u}_{M^{2+}} - \bar{u}_{H^+})\bar{x}_{M^{2+}} + F\bar{c}_{ex}\bar{u}_{H^+} \tag{28}$$

The evaluation of $\bar{c}_{ex}$, the fixed ionic site concentration in the membrane, may be achieved along different ways. In Ref. [22,23],

Table 4
Concentrations of exchange sites and absorbed sulfate ions in the membranes in contact with 0.5 N H_2SO_4 solution

Membrane	Water content (g/g of membrane)[a]	$\bar{c}_{ex} = \bar{c}_{ex}^{ph}$ (mol equiv./l)[a]	$\bar{c}_{ex} = \bar{c}_{ex}^{gl}$ (mol equiv./l)[a]	$\bar{c}_{SO_4^{2-}}$ (mol/l)[b]
CMS	0.27	8.15	2.1	0.030
CMV	0.22	9.80	2.1	0.015

[a] Estimated error ≈9%.
[b] Deduced from Fig. 5(a).

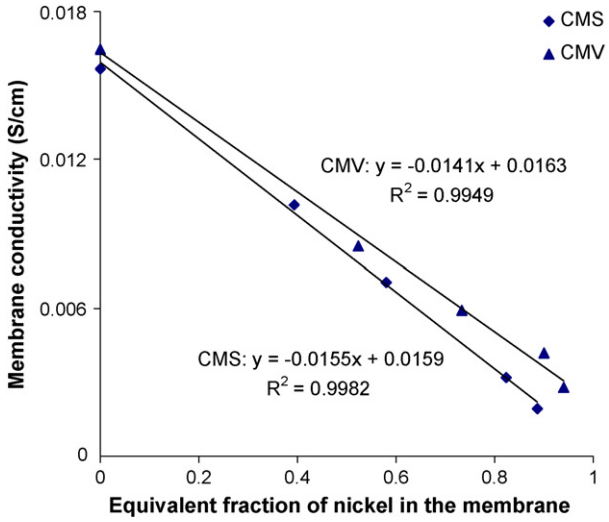

Fig. 9. Variation of membrane conductivity as function of equivalent fraction of Ni^{2+} in the membrane phase.

an estimate of this value was proposed based on the following definition:

$$\bar{c}_{ex} = \bar{c}_{ex}^{ph} = \frac{C_{ex} \times \rho_w}{W} \quad (29)$$

where C_{ex} is the exchange capacity (mequiv./g of dry membrane), ρ_w is the specific mass of water (g/cm^3). Because this definition of $\bar{c}_{ex}$ has a physical meaning by relating the ion concentration to the membrane water content, we use $\bar{c}_{ex}^{ph}$ to denote this value. The values are recorded in Table 4, by taking into account the values of C_{ex} and W in the case of a H_2SO_4 0.5 N solution (see Fig. 2).

Another definition for the concentration of fixed ion sites was proposed in the literature [16,20]. This was formulated as follows

$$\bar{c}_{ex} = \bar{c}_{ex}^{gl} = \frac{C_{ex}\rho_m}{1+W} \quad (30)$$

In this case, the notation $\bar{c}_{ex}^{gl}$ will be used for $\bar{c}_{ex}$ since in Eq. (30) the membrane is considered as a whole as a unique global phase. The values of $\bar{c}_{ex}^{gl}$ corresponding to our experimental systems are also recorded in Table 4.

Eq. (28) shows that the membrane conductivity changes linearly as a function of the equivalent fraction of nickel in the membrane. The straight lines obtained in Fig. 9 confirm the validity of Eq. (28).

The slopes of these straight lines and our results shown in Fig. 7 allow computing the value of the ratio $\bar{u}_{H^+}/\bar{u}_{Ni^{2+}}$. For the CMS membrane, this ratio is 39.8. In Table 5, this value is compared to the ratios of the hydrogen ion mobility to the mobility of other bivalent cations in the CMS membrane, as they have been reported in the literature [1,20]. The agreement between these values is extremely good. The experiments performed with the CMV membrane give a much lower value of the mobility ratio. For $\bar{u}_{H^+}/\bar{u}_{Ni^{2+}}$ we find a value of 7.4. This value reflects the fact that the CMV membrane does not manifest any appreciable specific permselectivity for monovalent or bivalent cations. We could find some similarity of this value with that obtained in other types of membranes that are also characterized by low permselectivity for mono- and bivalent cations. This is for example the case of Nafion® membranes, for which Pourcelly et al. [16] obtained a value $\bar{u}_{Na^+}/\bar{u}_{Ca^{2+}} = 5.0$ by using a conductivity technique.

Table 5
Hydrogen ion mobility compared to bivalent cation mobility in the CMS membrane

$\bar{u}_{H^+}/\bar{u}_{Ni^{2+}}$	$\bar{u}_{H^+}/\bar{u}_{Cu^{2+}}$ [a]	$\bar{u}_{H^+}/\bar{u}_{Zn^{2+}}$ [b]
39.8	37.9	38.7

[a] Ref. [1].
[b] Ref. [20].

Table 6
Diffusion coefficients of hydrogen ion and nickel in CMV and CMS membranes (10^{-11} m^2/s)

Membrane	$\bar{D}_{Ni^{2+}}$	$\bar{D}_{H^+}$	$\bar{D}_{H^+}$ [a]
CMS	0.13 ± 11%	5.3 ± 11%	5.1 ± 30%
CMV	0.58 ± 11%	4.3 ± 11%	4.9 ± 60%

[a] Ref. [24].

The Eq. (28) and the linear plots in Fig. 9 lead also to the determination of the hydrogen ion electrical mobility $\bar{u}_{H^+}$. In order to achieve this task we need to know the value $\bar{c}_{ex}$. On account of the concentration of fixed ionic sites $\bar{c}_{ex}^{ph}$, the values of $\bar{u}_{H^+}$ are respectively 1.7×10^{-5} and 2.1×10^{-5} cm^2/V s for the CMV and CMS membranes. With these values of $\bar{u}_{H^+}$ we have calculated $\bar{u}_{Ni^{2+}}$ and the diffusion coefficients of H^+ and Ni^{2+} as derived from the Nernst–Einstein relation:

$$\bar{D}_{H^+} = \frac{\bar{u}_{H^+}}{F} RT \quad (31)$$

The values obtained for the diffusion coefficients are shown in Table 6 and compared to values reported in the literature [24].

The alternative approach to evaluate $\bar{u}_{H^+}$ by introducing the definition of $\bar{c}_{ex} = \bar{c}_{ex}^{gl}$ yields diffusion coefficients of H^+ approximately equal to 2.0×10^{-10} m^2/s in the CMV and CMS membranes. With regard to these values it is worth mentioning that, by using also membrane conductivity measurements, Cherif et al. [20] found a value of 1.78×10^{-10} m^2/s for the CMS membrane.

3.6. The difference of ion-exchange and ion mobility in CMS and CMV membranes

The ion-exchange isotherms of Ni^{2+}–H^+ in presence of H_2SO_4 0.5 N are plotted in Fig. 7(a) and (b). These isotherms correspond to the substitution process of two H^+ ion-moles fixed on two neighbouring sulfonate sites by 1 mol of Ni^{2+}. We observe that the absorption expressed in mol equivalent of $Ni^{2+}$is somewhat larger in CMV than in CMS. From the initial slopes, α_{CMV} and α_{CMS}, of these two isotherms it follows that $\ln \alpha_{CMV}/\alpha_{CMS} \approx 0.38$. This yields an ion-exchange free energy for the CMS membrane about 1 kJ/mol less negative than for the CMV membrane. While this difference is small, the ion-exchange free energies actually are negative and large as proved by the ion-exchange isotherms depicted in Fig. 7. They show that, for a Ni^{2+}equivalent fraction reaching 0.5 in the external acid solution, the ion Ni^{2+}–H^+ exchange reaction is nearly complete in both membranes, the number of Ni^{2+} equivalent absorbed becoming almost equal to the membrane ion-exchange capacities (0.94 C_{ex} for CMV, 0.89 C_{ex} for CMS). The fact that the Ni^{2+}–H^+ exchange free energy is large in the case of both membranes may account for the linear pattern of the conductivities plotted in Fig. 9. In the experimental range of equivalent fractions of Ni^{2+} from 0 to 1 in the membrane, such linearity underlines the property of constant value of the Ni^{2+} mobility. This property suggests that, during the ion transport process, the substitution of bound H^+ by Ni^{2+} remains independent of the fraction of bounded hydrogen ions. However, as shown in Table 6, the Ni^{2+} ion mobility is much smaller than the H^+ mobility in both membranes and in CMS the Ni^{2+} ion mobility is about 5 times lower than in CMV. In order to advance some explanation for the relatively low mobility of bivalent metal ions it was suggested [25,26] that the double positive ionic charge entails a strong electrical interaction with

the negatively charged polystyrenesulfonate sites. The formation of ionic bridging of two adjoining sulfonate sites by these ions has also been called upon to account for the ion mobility lower values. Notwithstanding the importance of such strong interactions, which are ensuring the large values of the metal ion–hydrogen ion exchange energies, they are unable to explain the difference of Ni^{2+} mobility between the two membranes in presence of hydrogen ions. This becomes evident because of the nearly equal values of the Ni^{2+}–H^+ ion-exchange free energies found for the two membranes and the similarity of ionic mobility values of different bivalent metal ions, as shown for CMS in Table 5. All these transition metal ions exhibit different d electron configurations which, as known from coordination chemistry, should produce different forms of hydration and bonding. Let us recall that both the CMV and CMS membranes are made out of copolymers of styrene and divinylbenzene but their specifications differ by their degree of cross-linking due to the amount of divinylbenzene, the CMS presenting a higher degree of cross-linking. It was already suggested on ground of membrane swelling investigations (3) that, in presence of a 0.5 N. H_2SO_4 solution, the polystyrene sulfonate macro-ion conformation keeps in both membranes a retracted or coiled configuration. A similar poly-ion configuration as registered for H^+ could occur in the case of bivalent metal counter-ions strongly bound to the negatively charged sulfonate sites. A higher degree of cross-linking in CMS is expected to reinforce the rigidity of the poly-electrolyte conformation and to enhance the steric hindrance. These effects entail an increase of the activation energy of translocation from site to site involved in the hydrated metal ion transport process. The H^+ transport mechanism in water occurs by means of charge delocalization along hydrogen bridges. Because of the peculiarity of this mechanism the interference of cross-linking on the H^+ mobility is much weaker. We thus obtain large and only slightly divergent $\bar{u}_{H^+}$ values for the two membranes.

Bearing in mind that our membrane impedance measurements do not deliver information regarding the membrane surface, it is worth stressing that we are therefore unable to assess all the determining effects acting on the values of phenomenological parameters such as the membrane overall permselectivity of ion transport and the ion permeability. Evaluation of these parameters includes both the contribution of the ion mobility and the ion transfer across the membrane surface. Actually, by comparing these parameters between CMV and CMS, the role of the membrane surface is of paramount importance because of the CMS surface modification by a layer of positively charged polyelectrolyte [27,28], intended to slow down the transfer rate of bivalent cations.

4. Conclusions

In the case of CMV and CMS membranes, our conductivity results have confirmed, the validity of the micro-heterogeneity theory suggested by Zabolotsky and al. . . A slight modification of this model was however necessary in order to account for the data provided by the absorption isotherms. Measurements of these isotherms have led to introduce a partition of the electrolyte between the interstitial solution and external solution. We have also focused our attention on the Donnan equilibrium between the gel phase and interstitial phase inside the membranes.

We have proved that the membranes display an ideal permselectivity for the hydrogen ion and a high permselectivity for the other monovalent cations. The mobility of hydrogen ions determined from our conductivity measurements is equal to 1.7×10^{-9} and 2.1×10^{-9} $m^2/V\,s$, respectively for CMV and CMS membranes. The close similarity of these values seem to indicate that enhanced polystyrene cross-linking of the CMS membrane compared to the CMV membrane exert only small influences on the mechanisms determining the hydrogen ion mobility. With regard to such transport properties, the point can be stressed that the H^+ mobility relies essentially on the interactions occurring in the gel phase although the majority of absorbed salt and the quasi totality of absorbed acid are found in the interstitial phase. Enhanced cross-linking of polystyrene in ion-exchange membrane can however considerably affect the bivalent counter-ion mobility. This property is established from our selectivity and conductivity data of membranes in contact with a mixed solution H_2SO_4–$NiSO_4$. The ratio of the hydrogen ion mobility to the nickel ion mobility is about seven in the CMV membrane and 40 in the CMS membrane. Steric effects due to larger cross-linking in the CMS membranes play an important role by hindering the transport of large hydrated ions from site to site in the gel phase.

This study leaves open fundamental questions about the molecular mechanisms responsible for the ion selective transport inside polymer electro-membranes. Solving this problem is an essential task of further fundamental research that should take into consideration (a) the interactions of physical and chemical nature exerted by the charged sites; (b) the influence of the structure of absorbed water on ion interaction; and (c) the effects induced by the organisation of poly-electrolytes in macro-domains and their configuration changes in the gel phase as a function of the ion nature.

Nomenclature

A	membrane area (cm^2)
c_i	concentration of ion i in the external solution (mol/cm^3)
$\bar{c}_{ex}$	concentration (equivalents) of fixed charges in the membrane (mol/cm^3)
$\bar{c}_i$	concentration of ion i in the membrane (mol/cm^3)
$\bar{c}_{1ex}$	concentration (equivalents) of fixed charges in the joined-gel phase (mol/cm^3)
$\bar{c}_{1i}$	concentration of ion i in the joined-gel phase (mol/cm^3)
$\bar{c}_{2i}$	concentration of ion i in the interstitial phase (mol/cm^3)
C_{ex}	exchange capacity (mequiv./g of dry membrane)
d	membrane thickness (cm)
$\bar{D}_i$	diffusion coefficient of ion i in the membrane
f_1	volume fraction of the joined-gel phase
f_2	volume fraction of the interstitial phase
f_1'	volume fraction of the pure gel phase
$\bar{k}_{gel}$	equilibrium constant (see Eq. (8))
$\bar{K}$	coefficient of partition equilibrium between the external solution and the membrane
$\bar{K}_{gel}$	Donnan equilibrium constant (see Eq. (7))
$\bar{K}_{int}$	coefficient of partition equilibrium between the external solution and the membrane interstitial phase
$\bar{m}_{ex}$	experimental molality of absorbed acid ($mol/kg\,H_2O$ in the membrane)
m_s	molality of acid in the external solution (mol/kg)
$\bar{m}_{2s}$	molality of acid in the interstitial phase ($mol/kg\,H_2O$ in interstitial phase)
$\bar{m}'_{1i}$	molality of ion i in the pure gel phase ($mol/kg\,H_2O$ in pure gel phase)
$\bar{m}'_{2i}$	molality of ion i in the interstitial phase ($mol/kg\,H_2O$ in interstitial phase)

$\bar{N}_{H_2O}$	number of moles of water absorbed in the membrane per equivalent of fixed sites
$\bar{N}_s$	number of moles of electrolyte absorbed in the membrane per equivalent of fixed sites
$\bar{N}_{2s}$	number of moles of electrolyte absorbed in the interstitial phase per equivalent of fixed sites
R	membrane electrical resistance (Ω)
$\bar{u}_i$	mobility of ion i in the membrane ($cm^2/s\,V$)
W	membrane overall water content (g/g of dry membrane)
W_1	water content of the joined-gel phase (g/g of dry membrane)
$x_{M^{2+}}$	equivalent fraction of ion M^{2+} in the solution
$\bar{x}_{M^{2+}}$	equivalent fraction of ion M^{2+} in the membrane

Greek letters

κ^m	membrane specific conductivity (S/cm)
ρ_d	density of the dry membrane (g/cm^3)
ρ_m	density of the wet membrane (g/cm^3)
ρ_w	density of water in the membrane (g/cm^3)

References

[1] M. Siali, C. Gavach, Transport competition between proton and cupric ion through a cation-exchange membrane. I. Equilibrium properties of the system: membrane-$CuSO_4 + H_2SO_4$ solution, J. Membr. Sci. 71 (1992) 181–188.

[2] M. Boucher, N. Turcotte, V. Guillemette, G. Lantagne, A. Chapotot, G. Pourcelly, R. Sandeaux, C. Gavach, Recovery of spent acid by electrodialysis in the zinc hydrometallurgy industry: performance study of different cation-exchange membranes, Hydrometallurgy 45 (1997) 137–160.

[3] L. Xuan Tuan, M. Verbanck, C. Buess-Herman, H.D. Hurwitz, Properties of CMV cation exchange membranes in sulfuric acid media, J. Membr. Sci. 284 (2006) 67–78.

[4] L. Xuan Tuan, C. Buess-Herman, Study of water content and microheterogeneity of CMS cation exchange membrane, Chem. Phys. Lett. 434 (2007) 49–55.

[5] P.N. Gnusin, V.I. Zabolotsky, V.V. Nikonenko, A.I. Meshechkov, Development of the generalized conductance principle to the description of transfer phenomena in disperse systems under the acting of different forces, Zh. Fiz. Khim. 54 (1980) 1518–1522.

[6] V.I. Zabolotsky, V.V. Nikonenko, Effect of structural membrane inhomogeneity on transport properties, J. Membr. Sci. 79 (1993) 181–198.

[7] E. Volodina, N. Pismenskaia, V. Nikonenko, C. Larchet, G. Pourcelly, Ion transfer across ion-exchange membranes with homogeneous and heterogeneous surfaces, J. Colloid Interface Sci. 285 (2005) 247–258.

[8] A. Elattar, A. Elmidaoui, N. Pismenskaia, C. Gavach, G. Pourcelly, Comparison of transport properties of monovalent anions through anion-exchange membranes, J. Membr. Sci. 143 (1998) 249–261.

[9] J.H. Choi, S.H. Kim, S.H. Moon, Heterogeneity of ion-exchange membranes: the effects of membrane heterogeneity on transport properties, J. Colloid Interface Sci. 241 (2001) 120–126.

[10] S. Itoi, Electrodialysis of effluents from treatment of metallic surfaces, Desalination 28 (1979) 193–205.

[11] G. Pourcelly, A. Lindheimer, G. Pamboutzoglou, C. Gavach, Conductivity of sorbed hydrohalogenic acid in Nafion perfluorosulfonic membranes, J. Electroanal. Chem. 259 (1989) 113–125.

[12] C. Gavach, G. Pamboutzoglou, M. Nedyalkov, G. Pourcelly, AC impedance investigation of the kinetics of ion transport in Nafion® perfluorosulfonic membranes, J. Membr. Sci. 45 (1989) 37–53.

[13] K. Robberg, L. Dunsch, Electrochemical impedance spectroscopy on conducting polymer membranes, Electrochim. Acta 44 (1999) 2061–2071.

[14] G. Pourcelly, A. Oikonoumou, C. Gavach, H.D. Hurwitz, Influence of the water content on the kinetics of counter-ion transport in perfluorosulphonic membranes, J. Electroanal. Chem. 287 (1990) 43–59.

[15] G. Pourcelly, A. Lindheimer, C. Gavach, H.D. Hurwitz, Electrical transport of sulphuric acid in nation perfluorosulphonic membranes, J. Electroanal. Chem. 305 (1991) 97–113.

[16] G. Pourcelly, P. Sistat, A. Chapotot, C. Gavach, V. Nikonenko, Self diffusion and conductivity in Nafion^R membranes in contact with $NaCl + CaCl_2$ solutions, J. Membr. Sci. 110 (1996) 69–78.

[17] A. Chapotot, G. Pourcelly, C. Gavach, Transport competition between monovalent and divalent cations through cation-exchange membranes Exchange isotherms and kinetic concepts, J. Membr. Sci. 96 (1994) 167–181.

[18] A. Chapotot, G. Pourcelly, C. Gavach, F. Lebon, Electrotransport of proton and divalent cations through modified cation-exchange membranes, J. Electroanal. Chem. 386 (1995) 25–37.

[19] M. Taky, G. Pourcelly, A. Elmidaoui, Transport properties of a commercial cation-exchange membrane in contact with divalent cations or proton-divalent cation solutions during electrodialysis, Hydrometallurgy 43 (1996) 63–78.

[20] A.T. Cherif, C. Gavach, J. Molenat, A. Elmidaoui, Transport and separation of Ag^+ and Zn^{2+} by Donnan dialysis through a monovalent cation selective membrane, Talanta 46 (1998) 1605–1611.

[21] A. Chapotot, V. Lopez, A. Lindheimer, N. Aouad, C. Gavach, Electrodialysis of acid solutions with metallic divalent salts: cation-exchange membranes with improved permeability to protons, Desalination 101 (1995) 141–153.

[22] H.D. Hurwitz, R. Dibiani, Investigation of electrical properties of bipolar membranes at steady state and with transient methods, Electrochim. Acta 47 (2001) 759–773.

[23] H.D. Hurwitz, R. Dibiani, Experimental and theoretical investigations of steady and transient states in systems of ion exchange bipolar membranes, J. Membr. Sci. 228 (2004) 17–43.

[24] A. Heintz, E. Wiedemann, J. Ziegler, Ion exchange diffusion in electromembranes and its description using the Maxwell-Stefan formalism, J. Membr. Sci. 137 (1997) 121–132.

[25] T. Sata, Modification of properties of ion-exchange membranes. IV. Change in transport properties of cationexchange membranes by various polyelectrolytes, J. Polym. Sci. Polym. Chem. 16 (1978) 1063.

[26] T. Sata, T. Sata, W. Yang, Studies on cation-exchange membranes having permselectivity between cations in electrodialysis, J. Membr. Sci. 206 (2002) 31–60.

[27] T. Sata, R. et Izuo, Modification of the transport properties of ion exchange membranes. XII. Ionic composition in cation exchange membranes with and without a cationic polyelectrolyte layer at equilibrium and during electrodialysis, J. Membr. Sci. 45 (1989) 209–224.

[28] T. Sata, R. Izuo, K. et Takata, Modification of the transport properties of ion exchange membranes. IX. Layer formation on a cation exchange membrane by acid-amide bonding, and transport properties of the resulting membrane, J. Membr. Sci. 45 (1989) 197–208.